Experimental Characterization of Flexible and Soft Actuators for Rehabilitation and Assistive Devices

6

Daniel Gomez-Vargas, Felipe Ballen-Moreno, Orion Ramos, Marcela Múnera, and Carlos A. Cifuentes

6.1 Introduction

Several actuators have been developed for robotic devices, focused on assisting or enhancing the human limbs or joints. In this sense, considering both (1) the human limb or joint to assist and (2) the goal task, the actuators' energy should be efficiently provided to the user during the assistance process [1]. Therefore, to guarantee a proper human–robot interaction, multiple tests aimed at measuring and delimiting the device's functional capabilities should be carried out. Currently, this assessment has been commonly accomplished through experimental studies applied directly on subjects, either healthy or pathological. Notwithstanding, the test benches' inclusion in the characterization process could provide a general understanding related to (1) how the device interacts with the user and (2) what are its maximum capabilities.

Regarding the actuator type implemented on the device, the characterization process can evidence different techniques and the assessed variables. However, the goal of those processes remains focused on measuring the device's performance in the assisted activity. This way, characteristics such as the system response, stability, and device's limitations, among others can be measured to improve the robot behavior. Likewise, this characterization allows estimating accurate experimental

D. Gomez-Vargas
Biomedical Engineering, Department of the Colombian School of Engineering Julio Garavito, Bogotá D.C., Colombia

Institute of Automatics, National University of San Juan, San Juan, Argentina
e-mail: daniel.gomez-v@mail.escuelaing.edu.co

F. Ballen-Moreno · O. Ramos · M. Múnera · C. A. Cifuentes (✉)
Biomedical Engineering Department of the Colombian School of Engineering Julio Garavito, Bogotá, Colombia
e-mail: felipe.ballen@mail.escuelaing.edu.co; orion.ramos@mail.escuelaing.edu.co; marcela.munera@escuelaing.edu.co; carlos.cifuentes@escuelaing.edu.co

169

models, starting from the actuator or the device coupled in the application, which can be used to enhance the control strategies and consequently the human–robot interaction.

As mentioned before, the methodologies to measure the device's capabilities commonly have been divided into experimental tests (1) within the goal application (i.e., involving users) and (2) through test bench setups. Furthermore, depending on the stage of the actuator's development, this assessment could include different previous tests. For instance, in *Fang et al.*, the initial phases of a pneumatic bending actuator were focused on determining an analytical model and building an actuator's prototype [2]. Subsequently, the actuator was characterized using a test bench structure based on the device's application, and then it was assessed in the goal users. In the same line, another study presented the characterization of an ankle exoskeleton based on a variable stiffness actuator, focusing on measuring the device capabilities in terms of bandwidth, system response, assisted torque, and saturation non-linearities for different stiffness values [3].

On the other hand, the characterization process can also include complex variables aimed at the device's specific application. For instance, *Yandell* et al. [4] defined an analytical kinetic model to estimate the energy losses of a powered ankle–foot orthosis based on cable-driven actuators. For this case, the proposed assessment included experiments applied directly to subjects.

In this context, this chapter presents the characterization of two types of actuators focused on rehabilitation scenarios, showing the trends and essential variables measured in the experiments. The first actuator consists of an ankle exoskeleton based on variable stiffness' concepts detailed in Chap. 7, and the second actuator describes a soft hand exoskeleton based on pneumatic actuation concepts.

6.2   Characterization of Actuators

The importance of understanding the actuators' capabilities arises from the motivation to enhance the device's performance and improve the human–robot interaction. However, considering the goal user and the desired scenario, the assessed variables change depending on the actuator type. In this sense, the following sections present the trends and essential variables according to the actuator principle, addressing an experimental characterization of a variable stiffness actuator and a soft actuator based on pneumatic principles.

6.2.1   Characterization of a Variable Stiffness Actuator in Gait Rehabilitation

Different actuators for assistive scenarios (e.g., pneumatic, hydraulic, electric actuators) were presented in Chap. 2. This way, aspects such as the actuator type and the assisted joint involve determining (1) what should be the proper amount of energy provided to the user during the task and (2) how this energy should be provided [3]. Concerning the variable stiffness actuators, devices based on this

actuation type allow changing the system behavior to be adapted to the user's physical conditions, as Chap. 7 shows. Therefore, those devices could exhibit multiple responses affecting the control performance.

In this sense, this actuation type requires a complete dynamic and static model that describes the system behavior under the goal application. Nevertheless, some devices could have complex mechanical designs, resulting in intricate models. Hence, a characterization process could simplify the model being delimited within the conditions where the device should operate. Moreover, this process could also provide information about the device performance and physical interaction in those scenarios.

6.2.1.1 Trends and Essential Variables

In general terms, robotics aimed at gait rehabilitation integrate principles applied in passive orthotic structures, although incorporating benefits such as the capacity of providing torque, feedback during the assistive process, modification of the device performance, consistency during the exercise, and support for the therapists, among others [5]. From the motivation to enhance the physical interaction during the assistance, compliant actuators are emerging as a solution to preserve the device's actuation system and improve the transparency effect during an interaction forces scenario. Particularly, series elastic actuators and variable stiffness actuators are being exhibited as potential principles.

Robotic devices based on variable stiffness actuators are widely recommended in applications where the robot interacts intensively with the human [6, 7] because of advantages evidenced by this principle under rehabilitation scenarios, as Chap. 7 presents. Specifically, a variable stiffness effect enables the device to modify its behavior considering the desired physical interaction. Moreover, from the bioin- spired concepts applied in assistive robots, variable stiffness resembles the motor human functions. Those devices aim at assisting the lower limb joints' sagittal plane (i.e., hip, knee, and ankle). However, each one of these joints has challenges related to the required torque, movements on the other planes (e.g., add–abduction and internal–external rotation), reaction forces, and torque transmission, among others.

In the ankle rehabilitation context, powered ankle–foot orthoses have applied this actuation type, exploiting the spring's inclusion characteristics, i.e., shock loads and backdrivability. This way, kinematic and kinetic models for control purposes could be complex, and additionally, they could not provide information related to the environmental constraints and users' requirements. Thus, an experimental characterization, using a test bench either static or dynamic, or through human trials, is exhibited as an alternative to determine these aspects [1, 8]. For a static setup, the structure fixes the actuators' output (see Fig. 6.1), restricting their motions and coupling sensors to measure the interaction forces and the device performance [8]. The actuators execute the set-point values resembling the device's application and inducing a physical effect in the output (i.e., torque, force, pressure, angular or linear position). This way, it can be understood the actuator capabilities (i.e., apparent bandwidth, peak, and continuous torque), adjusting different controllers to reduce
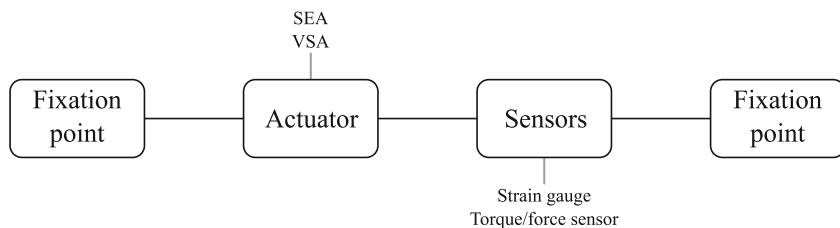
Fig. 6.1 Descriptive scheme of the principal components for a static bench
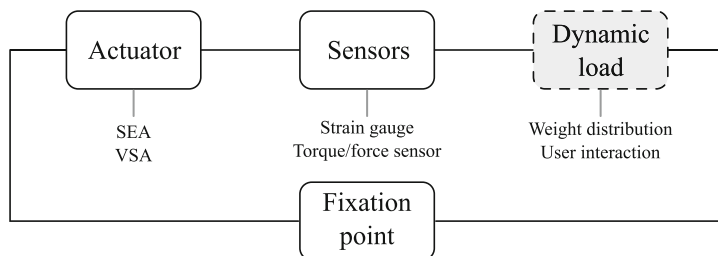

Fig. 6.2 Descriptive scheme of the principal components for a dynamic bench

position or torque errors, increase the time of response. Nevertheless, it does not represent its actual performance during operation [9].

On the other hand, a dynamic test bench intends to closely assess the actuator in the application, including the user's external forces. In contrast to a static test bench, the actuators' output is coupled to a dynamic load [10] (see Fig. 6.2). This way, the trials could recreate a realistic scenario, including the user's dynamic that affects the device's performance (i.e., bandwidth and temporal response).

6.2.1.2 T-FLEX Design and Test Bench Structure

T-FLEX is a wearable and portable ankle exoskeleton based on variable stiffness actuators (see Chap. 7) to assist the dorsi–plantarflexion movements without restricting the other ankle motions [11]. This ankle exoskeleton comprises two servomotors attached to bioinspired tendons (see Fig. 6.3) whose mechanical behavior is similar to the human Achilles tendon [12]. T-FLEX integrates a bidirectional system of stiff filaments to (1) involve both actuators during the assistance process and (2) correct the foot pathological postures. Additionally, this device is manually adjustable and usable for both limbs.

For the variable stiffness effect, passive elements resemble the stiffness of a human tendon as a spring-like component. Thus, T-FLEX integrates a braided material formed by (1) elastic filament (Filaflex, 2.85 mm, Recreus, Spain) and (2) fishing rod (eight filaments, Sufix 832, USA). These filaments were intertwined following a volumetric fraction of 14% to accomplish a variable stiffness performance regarding the elongation.
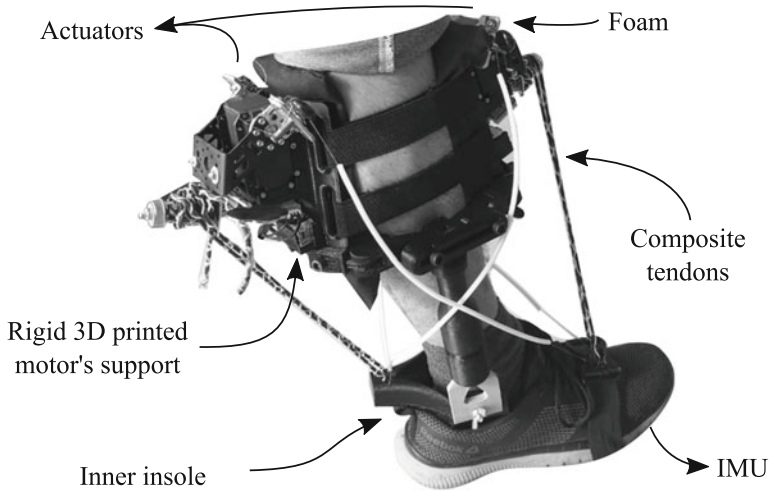
Fig. 6.3 Wearable and portable ankle exoskeleton T-FLEX. The remarked elements refer to the main parts of the device

In terms of functionality, T-FLEX includes two operational modes, i.e., (1) stationary therapy and (2) gait assistance, which employ a calibration stage customized for each user. For the first modality, the exoskeleton executes dorsi–plantarflexion repetitions, integrating an inertial sensor placed on the foot tip to detect the user movement intention. The implemented therapy model allows varying parameters such as the repetition number, repetition frequency, and movement speed. This modality has exhibited promising outcomes in a rehabilitation context with a stroke patient [13].

For the gait assistance, T-FLEX assists the user's gait phases (i.e., mid-stance, heel-off swing, and heel strike), providing dorsi–plantarflexion movements and increasing the system stiffness, following the actuators' combination shown in Fig. 6.4. In this sense, the device incorporates a gait phase detector based on a hidden Markov model and machine learning [14], detailed in Chap. 5. A preliminary study focused on assessing the T-FLEX's actuation system in a walking application evidenced significant potential for the lower-limb kinematics of patients who suffered a stroke [15].

From the T-FLEX's design and goal applications presented above, the test bench structure employed to characterize the device should consider different conditions that affect the device response and performance. Thus, the user's anthropometric measurements play a significant role in the torque provided by the exoskeleton. Specifically, the distance between the ankle and the fixation points of the tendons (i.e., plastic part placed on the foot tip and the structure adapted to the heel), the shank's length, and the user's body composition modify the torque provided to this joint (see Fig. 6.5). Additionally, the ankle torque, tendon force, and the electrical
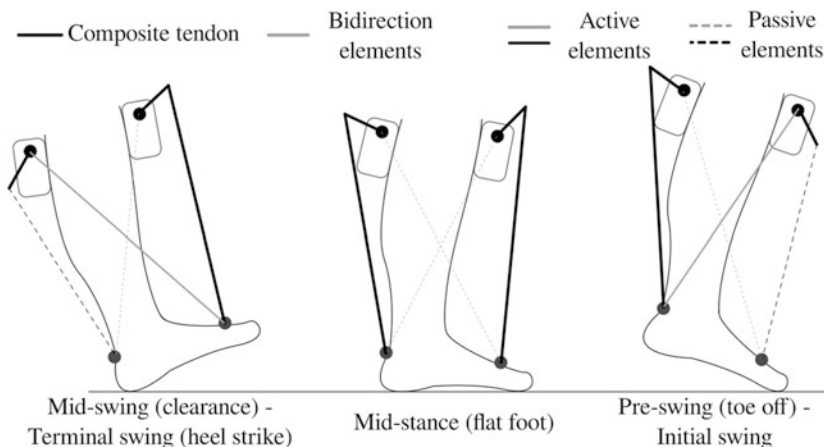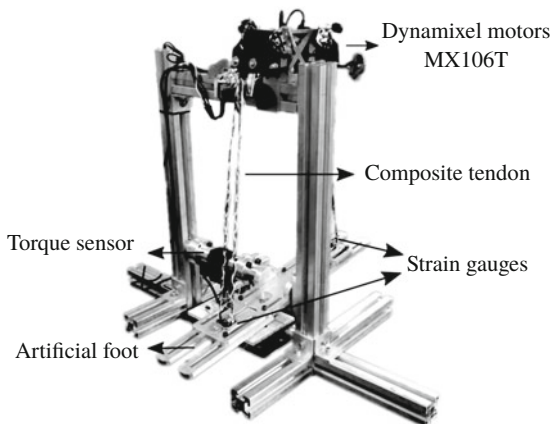
Fig. 6.4 Descriptive scheme of the mechanical configuration of the T-FLEX's functionalities

Fig. 6.5 Description of the test bench showing the principal components of the test bench, illustrating sensors, actuators, and principal dimensions that represent the human shank and ankle joint

and physical characteristics of the T-FLEX's actuators are the main variables in an experimental process that could assess the device's performance.

In this context, a mechanical structure composed of aluminum frames was developed to adjust the variable distances mentioned above, applying the T-FLEX's operation concept in an actual application (see Fig. 6.5). This test bench structure included a torque sensor FY01 (Forsentek, China) coupled on the artificial ankle and a set of strain gauges (RS PRO, UK) placed on the tendons' fixation points. For the actuators, 3D printed pieces fixed the smart servomotors to the mechanical structure, resembling the shape of a human shank.

6.2.1.3 Experimental Procedure

Firstly, the experimental procedure intended to analyze the tendon behavior resembling the T-FLEX operation principle. For this purpose, a tensile test was carried
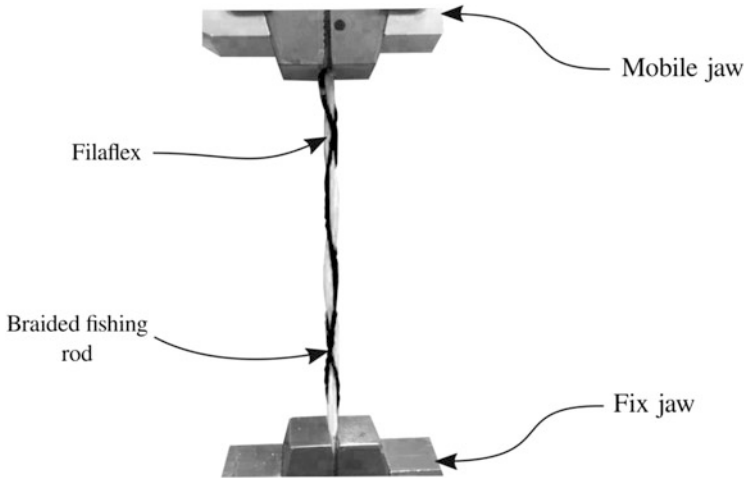
Fig. 6.6 Tensile test experimental setup to measure the T-FLEX's tendons behavior

out through a universal machine, fixing a specimen between two jaws, as shown in Fig. 6.6. Besides, the tensile tests followed the ASTM C1557-14 [16].

On the other hand, considering the T-FLEX variability, the second part of this characterization analyzed the tendon effect under a pretension level of 10 N in an assistance process. The selected force level corresponds to the medium force concerning the maximum value that induces actuator saturation. From this value, the study included two signals to measure the device response and estimate the device capabilities (i.e., step and chirp). These signals were sent to the actuators as position commands with an amplitude between 3 and 15 degrees, which is a common value applied in an actual application. Likewise, the set-points resembled the T-FLEX operation in a gait assistance application, following the movements presented in Fig. 6.4.

6.2.1.4 Results

From the tendon trials, stress–strain tests estimated two elastic zones and their Young's modulus, as Fig. 6.7 shows. A range of strain defines each zone: zone A between 0 and 0.10 mm/mm and zone B between 0.1 and 0.15 mm/mm. Nevertheless, zone C presented inconsistent stress values and rupture point. However, this last zone is not taken into account in the analysis because the bioinspired tendons will be loaded with forces smaller than the required for the rupture point.

On the other hand, considering the assistance application in the proposed test bench structure, the step function measured both the response of the T-FLEX's actuation system and the behavior of the composite tendons under tension. Figure 6.8 shows the curve obtained during the dorsi–plantarflexion movements in terms of the assisted torque and tendons force. The first set-point (i.e., segmented black line) describes the dorsiflexion command. In this movement, the anterior motor turns
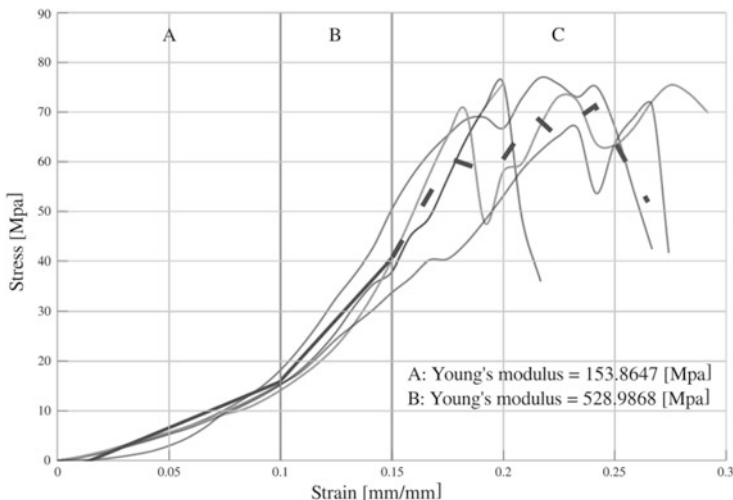
Fig. 6.7 Tensile results of the bioinspired tendons. The stress–strain curve presents the Young's modulus for the A and B zones

to pull the foot, and the posterior actuator works reversely. This way, the system transmits positive torque to assist the ankle. For the second set-point, the actuators operate in opposite directions concerning the movement mentioned above. Thus T-FLEX assists the plantarflexion, providing negative torque on the ankle joint.

The chirp signal measured the system response to frequency changes and the maximum values of torque on the ankle for the different amplitude values. Figure 6.9 shows the system behavior in terms of torque on the ankle, the tendons force, and T-FLEX's actuators. The responses illustrated in Fig. 6.9 occurred in the tendons-alone configuration for the dorsi–plantarflexion movements with a force level of 10 N.

Considering the obtained responses, the trials reported that T-FLEX exhibits a bandwidth close to 6.8 Hz for the measured amplitude range. This value was estimated using the system identification toolbox of MATLAB (MathWorks, US). Likewise, the maximum provided torque measured on the ankle was 12 Nm for propulsion and 20 Nm for the dorsiflexion movement. In terms of the system response, the trials evidenced (1) a delay related to the tendon elasticity (i.e., close to 45 ms) and (2) a stabilization time less than 284 ms. In general terms, T-FLEX can assist the human gait under this configuration. However, the control architecture should include an adaptive stage that accelerates the device response concerning the set-point value and the pretension level. This way, the device could anticipate the stabilization time and the tendon delay, ensuring the maximum torque transmission in the specific gait phase.
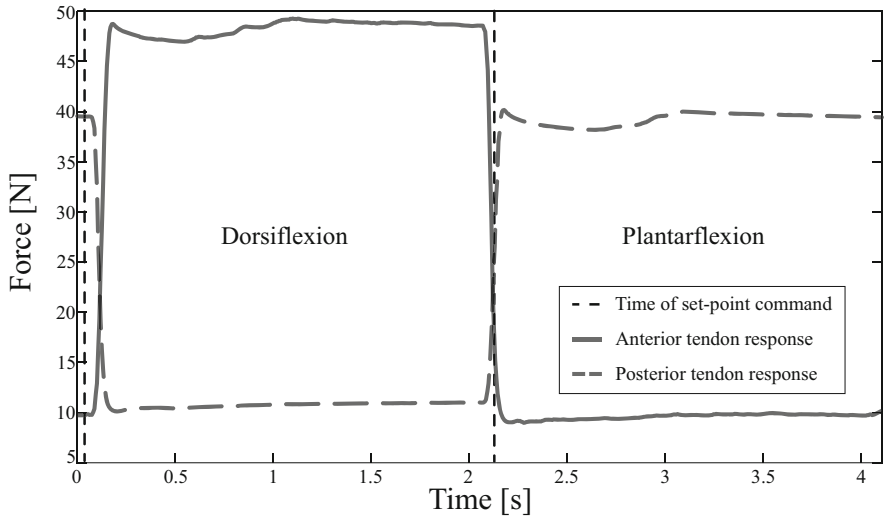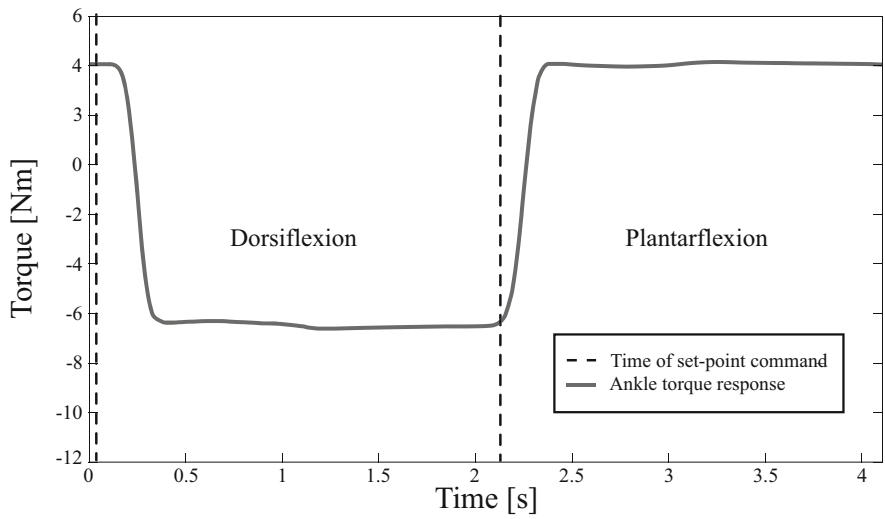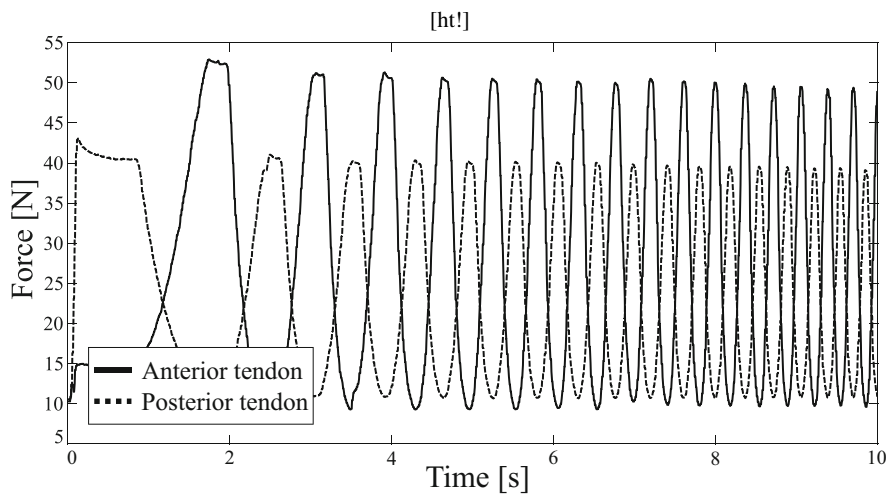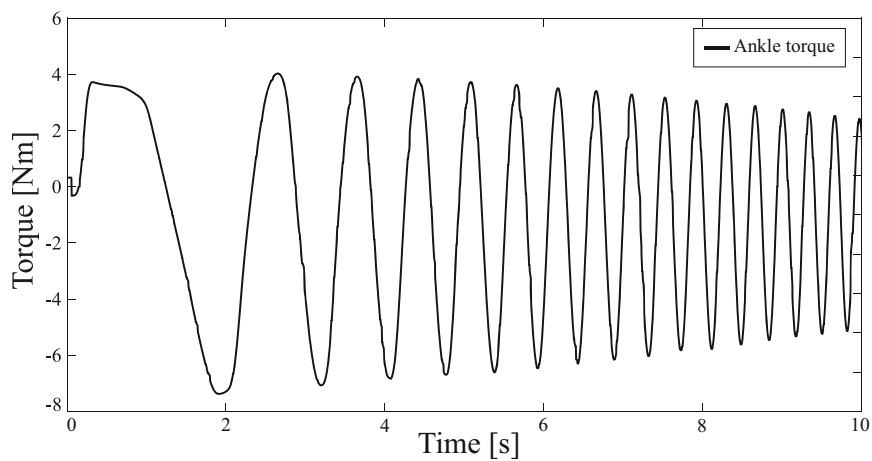
Fig. 6.8 Step response of the system for the dorsi–plantarflexion movement. (**a**) Force outcomes.
(**b**) Torque outcomes

(a)

(b)

Fig. 6.9 System responses for the chirp signal in the tendons-alone configuration executing dorsi–plantarflexion movements under a force level of 10 N. (**a**) Force outcomes. (**b**) Torque outcomes

6.2.2   Characterization of a Soft Actuator Based on Pneumatic Actuation in Hand Rehabilitation

New technologies in the engineering field have raised new design paradigms such as soft robotics strategies. These technologies are differentiated by using soft materials such as elastomers or flexible fabrics such as lycra. These techniques facilitate assistive or rehabilitative devices by eliminating mechanisms that require exact alignment of the limb joints with the degrees of freedom of the device [17]. This is possible because these types of soft actuators do not have defined degrees of freedom; on the contrary, they are considered to have infinite degrees of freedom [18].

Another advantage proposed by this new technology is the separation of the actuation source from the device attached to the person. This is to reduce the weight that the limb to be assisted or rehabilitated must support. Usually, systems are built to be stored in a backpack or control box apart from the device. These properties of systems built using soft robotics make it possible to reduce the device's weight concerning rigid technologies considerably. However, modeling and mathematically characterizing actuators based on pneumatic actuation are considerably more complex than performing this procedure on electric actuators or DC motors due to the non-linearities that pneumatic systems can generate and their infinite degrees of freedom.

6.2.2.1 Trends and Essential Variables

As seen in Chap. 2, the amount and form of motion of each degree of freedom of a robot allow finding the kinematic model to the robot. However, in actuators based on soft robotics techniques, it is impossible to perform these calculations due to their high deformation properties. In these cases, it is usual to characterize the relevant variables of the problem to be solved with the actuator through experimental techniques [19, 20]. In other cases, computational models based on finite element analysis [21, 22] are used. In this section, characterization methodology of soft actuators to be used in an upper-limb exoskeleton will be explained. Therefore, the relevant variables must be related to this problem.

Since a hand exoskeleton developed for assistance or rehabilitation is a wearable system that must be comfortable for the user, the most relevant variables in this application will be those that achieve the assistance of the human hand. These variables are the range of motion and the forces needed to intervene in the movements of the fingers without affecting comfort and efficiency. Specifically, the requirements for the design of a hand rehabilitation or assistive device according to the state-of-the-art review are divided into different categories. One of these is practical considerations, such as the number of fingers to be assisted, the device's weight, and its dimensions.

The other category focuses on the kinematic requirements necessary for the device to be considered functional in clinical rehabilitation or assistive applications. This category defines the ranges of motion and forces required for each actuator

of the exoskeleton, as mentioned above. Finally, the control category specifies actuator response speed, system bandwidth, and device sensing. For each of the categories, values and requirements are defined based on engineering studies and clinical recommendations.

In the category of general considerations, the wearable device's total weight should not exceed 3 kg. The weight supported in hand should be around 0.5 kg [23], and the actuator dimensions should be in the range of human fingers' size. In terms of kinematic requirements, each actuator must bend at least 250° to be considered capable of assisting in human finger flexion [23]. The force to be exerted by the actuators establishes that forces higher than 7 N allow any assistance in daily life tasks [23]. However, only 3 N is enough to generate practical assistance for rehabilitation cases [17]. In the control section, the sampling rate should be at least 20 times faster than the response speed of the actuators [23]. The actuators' speed should be around the human hand's average values, which is 0.3 m/s [24]. Finally, the system must be powered by a small power supply and air supply while avoiding exceeding the total allowable weight.

Since the general considerations and control category's characterization are usual in engineering fields, they will not be explained in detail. Measuring the device's weight and actuators does not involve any complexity, although it gives relevant information. Similarly, calculating the system's sample time is not part of the actuator characterization and becomes a requirement of the complete device; in this case, only the actuators will be studied. The kinematic requirements category is the one that will be detailed in this section. In this category, variables such as the pressure required to generate the maximum bending and the force that the soft actuators can generate are mentioned.

To evaluate the necessary pressure required to generate actuator bending, a test is performed that relates air pressure measured with air pressure sensors to the maximum actuator tip bending angle measured by video processing. A comparative test of actuator tip pressure versus actuator tip angle reported that it is possible to achieve mean bending at pressures in the range of 42 kPa to 52 kPa depending on actuator length. In that study, silicon actuators built using the PneuNets technique were compared. The values were rectified with finite element analysis simulations specializing in this type of actuator [25]. Another comparison of silicone actuators was performed. It was found that the fiber reinforced-type actuator of Elastosil M4601 material with a length of 16 cm achieves full bending at 243 kPa [26].

Moreover, a study was conducted to identify how construction parameters, such as actuator length, internal air chamber inner radius, and actuator wall thickness, affect the pressure required to achieve full bending. It was concluded that the smaller the actuator length and internal radius, the higher the pressure must be to achieve full bending. Also the chamber wall is directly proportional to the required pressure, so the thicker the actuator, the higher the pressure must be to achieve full bending. The comparison actuator in the study has a length of 16 cm, a wall thickness of 2 mm, and an inner radius of 8 mm. With this actuator, full bending is achieved at 200 kPa (approximately 30 psi) [27]. Finally, silicone actuators achieved medium bending (close to 90 degrees bending) at a pressure of 110 kPa. It was also shown that the

actuator reduces this angle if attached to a finger simulating an exoskeleton [28]. As seen in these studies, varying the actuator dimensions, the material of construction, and the type of reinforcement changes the actuator behavior for the required input pressure that generates the maximum bending.

On the other hand, several ways to find the force generated by soft actuators have been studied. The most common ones are based on measuring the actuator tip force with a load cell. Two configurations are regularly presented to measure the force exerted on the actuator tip. One measures the bending force. The other configuration measures the blocked force, which is greater than the bending force. Some studies report bending average force values close to 4.5 N at 407 kPa in silicone actuators with a length of 80 mm. In that study, different silicone actuators of different lengths are compared. It is evident that shorter actuators generate more force, e.g., a 60 mm long silicone actuator reaches the maximum force (5.58 N) at 450 kPa [29]. Another study using hydraulically actuated fiber reinforced silicone actuators can generate bending forces of 9N at the tip of the actuator [30]. Silicone actuators were compared for use in rehabilitation or assistive hand devices. In that study, bending force values were obtained for actuators of different elastomer references. Thus actuators constructed with Dragon-skin 10 achieved a force of 3.19 N at 180 kPa and actuators constructed with Dragon-Skin 20 reached 3.5 N at 380 kPa [19].

Moreover, the blocked force test has been used more frequently to characterize this actuator, so more information is available for comparisons. The force recorded in this test is usually higher than that recorded in the bending force test. For example, a 13 cm long PneuNets silicone actuator generates a blocked force of 1.2 N at only 43 kPa [25]. In fiber reinforced actuators, blocked force values of 1 N at 200 kPa were reported for Dragon-Skin 10 silicone. Furthermore, for references such as Elastosil M4601, forces of 5 N were obtained at pressures of 400 kPa. These actuators were constructed with a length of 17 cm [26]. Likewise, for these same types of fiber reinforced actuators, force values close to 8.8 N at 180 kPa were achieved for materials such as Dragon-Skin 10 and 9.96 N at 380 kPa for Dragon-skin 20 [19]. Finally, in 2017, forces of 9.12 N at only 120 kPa were achieved in a hybrid silicone and textile actuator [20].

As presented above, performing experiments where peak forces, efficiency, and kinematic variables are determined is the easier way to obtain the device's models. Fiber reinforced- and textile-type actuators with pleats have been the most developed and used in hand assistance and rehabilitation applications to create new exoskeletons based on soft robotics [31, 32]. Therefore, comparing them experimentally is relevant to select the most efficient one. Starting from the premise of designing a wearable device for hand assistance and rehabilitation, test benches were designed for fiber reinforced- and textile-type actuators with pleats characterizing the efficiency of the two types of actuators and another test bench to find the bending force and blocked force that these actuators can generate.

6.2.2.2 ExHand Design and Test Bench Structure

Based on how the behavior of soft actuators is evaluated according to state of the art, three types of tests were performed for a textile and a silicone actuator. According
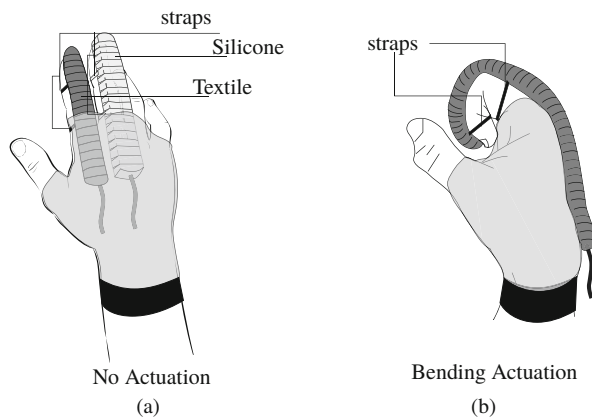
straps
Silicone
Textile
straps

No Actuation
(a)

Bending Actuation
(b)

Fig. 6.10 Diagram of actuators' locations. (**a**) Possible placement of the soft actuators to create the assistive or rehabilitative hand device. (**b**) Demonstration of how the bending actuator generates the assisting motion on the human finger

to the designs that have been made, the ExHand actuators' location on the hand can be seen in Fig. 6.10a. The figure also shows how the actuator's bending motion allows the bending of the fingers without concern for the degrees of freedom of the actuator Fig. 6.10b. These actuators are very different from each other in terms of dimensions, materials, and construction methods, so each actuator's characteristics will be explained in general terms.

The silicone fiber reinforced actuator is built by pouring elastomeric materials such as silicone into 3D printed molds. Depending on the type of motion generated, reinforcements are made with rigid elements such as layers of carbon fiber layers and inelastic thread [27]. The type of movement that was evaluated is elemental bending. This motion works to simulate human fingers in assistive or rehabilitative applications in a hand exoskeleton. The fiber reinforced actuator built to explain this section was made with an elastomer (Dragon-Skin 00–30 from Smooth on). The entire construction process can take about two days, as the silicone must cure in the molds. One of the features that these actuators can provide is based on the fact that a single actuator can be configured to generate different movements, such as bending, extension, and torsion. However, it should be noted that this later construction cannot be modified, and the actuator will always have the same behavior. An example of this property is a thumb actuator's design, which integrates different motions into a single actuator [33].

On the other hand, the textile actuator uses elastic and inelastic fabric materials for the creation of the bending motion and an elastic–plastic element (Stretchlon 200, FibreGlast) to contain the air internally. The construction process consists of sewing a layer of rigid fabric with a layer of elastic fabric, creating a finger-sized pocket. This layer must be sewn together, generating pleats that facilitate the bending motion [34]. The construction time of a textile actuator with pleats for the
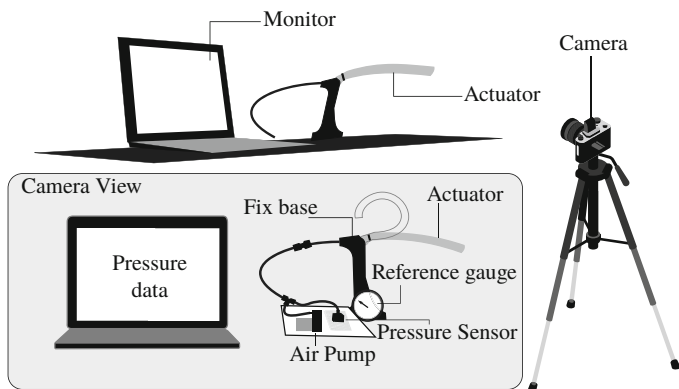
Fig. 6.11 General setup and parameters displayed through the camera for the test bench where the bending angle measurement concerning the input pressure is performed

bending motion can take about 6 h. The advantage of this type of actuator is that it can generate different motions. However, in contrast to silicone actuators, these can be actuated independently, generating actuators with bending and extension movements with independent control [34]. From the ExHand design presented previously, Fig. 6.11 shows the test bench setup developed for the experimental characterization.

6.2.2.3 Experimental Procedure

An experiment was designed to measure the pressure required by the actuators to generate the maximum bending angle to characterize the actuators' efficiency. This variable is the angle required when the actuator is used to assist in closing the human hand. An ASDXACX100PAAA5 analog pressure sensor (Honeywell, USA) and a D2028 air pump (Karlsson Robotics, USA) were used for this purpose. To define when the actuator reaches the maximum bending angle, the open-source video post-processing software Kinovea was used. For this purpose, the entire experiment was recorded at 30 FPS ensuring that the camera scene takes the actuator's motion and the data provided by the microcontroller display. The critical data to synchronize the video and microprocessor values were the time, the number of samples, and the sensor's pressure. The processing speed of the microprocessor was synchronized with the 30 FPS of the video. For each actuator, five repetitions were performed, which consisted of moving the actuator from steady state (no air pressure) to maximum deflection employing the air pump.

Other variables that could be obtained to study the actuators' behavior could include the actuation speed, acceleration, and even bending shape or path trajectory. All this information can be obtained in the same test bench of Fig. 6.11 using the Kinovea software (Kinovea org, France). This software uses artificial vision methods to process some marker changes in each video frame and estimate the variables listed above.

Fig. 6.12 Bending force test bench assembly where the necessary elements can be seen. Here the distance from the sensor and the height of the actuator base are variable to redirect the actuator tip and achieve that the force is applied correctly on the sensor
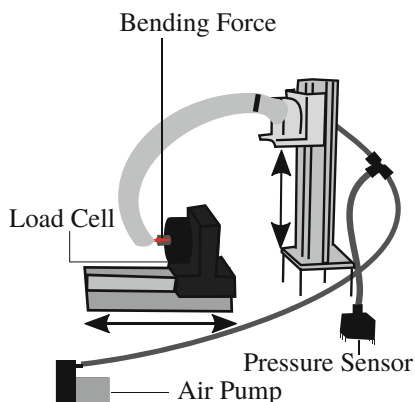
The two types of forces that the actuators can generate at the same pressure were measured. The bending force, which consists of measuring the force generated by the tip of the actuator when it reaches the maximum bending [29], was the first experiment. Moreover, the second one was the blocked force. This test consists of restricting the actuator's bending motion using a rigid sheet and measuring the tip force [19]. In both cases, the air pressure used was that which in the previous experiment achieved maximum bending. The instrument used to measure the actuator force was an FC2211-0000-0010-L load cell (TE Connectivity, Switzerland). Fig. 6.12 shows the test bench for performing the maximum bending force measurement. As in the first experiment, five repetitions were performed for each actuator, which was averaged to estimate the applied force. In this experiment, the two crucial variables (input pressure and force) are acquired by the microcontroller, so it is unnecessary to synchronize video data with sensor data. Since the two types of actuators have different behaviors in their bending path trajectory, the test bench must change the height and the distance at which the force sensor is located.

The experiment to measure the blocked force uses the same elements. It is based on the same five repetitions of pressurizing the actuator with the pressure that generates full bending and recording the force values at that point for each actuator. The set-up in Fig. 6.13 is the one that represents the test bench for this experiment. In this case, neither the height nor the distance needs to be modified. In this case, the two actuators are constructed of the same length.

6.2.2.4 Results

The pressure required for the actuator to achieve full bending was measured. The five values were summarized by the mean and their standard deviation to be plotted and compared in Fig. 6.14. In this graph, the comparison of the pneumatic energy required to perform the same task for the two types of actuators can be seen. Note that the textile actuators reach the maximum bending angle at a value of 11.04 psi (76 kPa). And the silicone actuators at a higher value of 28.49 psi (196.4 kPa). It is important to note that both systems reach the full bending angle at air pressure below

Fig. 6.13 Test bench setup to perform the blocked force test. The figure shows how the top layer restricts the bending motion and allows redirecting the force to the actuator tip
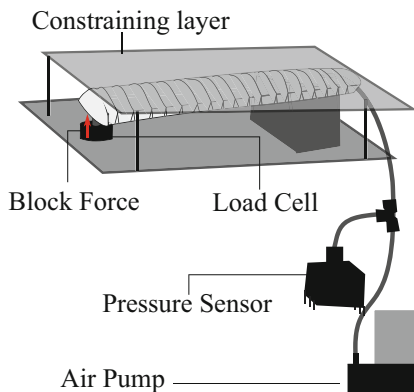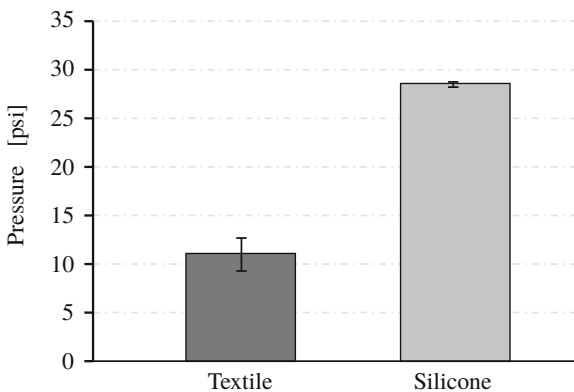

**Fig. 6.14** Air pressure needed to achieve full bending performance for both types of actuators

200 kPa. This indicates that both types of actuators can be used with small size and low-power air sources. Nevertheless, the difference between the results of textile actuators and silicone actuators is high. It can be affirmed that textile actuators are more energy efficient in achieving the maximum bending angle. In other words, the silicone actuators, while meeting the test objective and the stated requirements, are less efficient than the textile actuators. This means that silicone actuators require more air pressure to perform the same task as textile actuators.

It is vital to identify that the deviation of the textile actuators' data is higher than in the silicone actuators. In this sense, silicone actuators are more stable and accurate of the input pressure required to achieve full bending. However, considering the purpose of those devices, the found deviation is not relevant. Suppose the actuator is pressurized with the highest value of the five values found. In that case, it is assumed that the actuator will be in the position of full bending.

The experiments that found the actuator forces are shown in Fig. 6.15. As with the previous results, the graphs represent the means and deviations of the five values found in the test. It is possible to observe how the bending force for the two actuators is very similar. In comparison, in the blocked force test, there are

Fig. 6.15 The force
generated by the actuators
according to the two different
setup and the comparison full
bending pressure
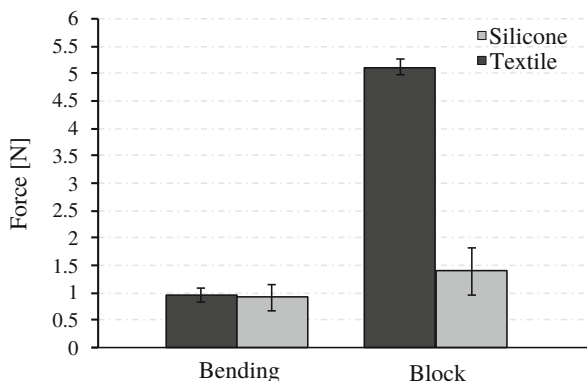
pretty high differences between the two actuators. In detail in the bending force test
performed, very similar results were obtained regarding the force exerted.

The textile actuators generated an average peak force of 0.95 N at 11 psi, and the
silicone actuators 0.92 N at 28 psi. These values are very close to each other. There
is no difference between the two actuators in this type of experiment. Therefore, it
can be said that the two types of actuators generate the same bending force at the
maximum bending position. The difference is in the pressure required to generate
this value. If the force exerted at the actuator's tip at the same input pressure is
compared, a lower value would be seen in the silicone actuators. With this test, it is
rectified that the textile actuators are more efficient than the silicone actuators.

The blocked force test results show that the textile actuators generate more force
than the silicone actuators. In this case, the textile actuators generate 5.1 N of locked
force, much higher than the 1.4 N of the silicone actuator. Another critical point seen
in Fig. 6.15 is the deviation of the fiber reinforced-type silicone actuator's data. In
both the bending force test and the blocked force test, the data are more scattered in
this actuator type. This may be related to the fact that silicone actuators' behavior in
terms of actuator tip forces is less repeatable and more complex to control than in
textile actuators.

Knowing the application for which the two types of actuators are intended to
be used and the design requirements stated in state of the art is easy to establish
which are the most feasible results according to each test. For example, in the first
experiment, the actuator needs less pressure to achieve full bending and, therefore,
reduce the power source's size, and the air source is desired. All this reduces the
device's weight, which is an essential factor in wearable devices for assistance or
rehabilitation [33]. According to the results obtained, textile actuators are better than
silicone actuators for the pressure required to achieve the entire bending movement.
So in the design of a wearable assistive or rehabilitation device, they should be
considered over silicone actuators.

Similarly, the results of the force tests are analyzed in these cases. For this type
of application, the desired results are the higher force values. The more force the
actuator can generate, the more possibilities it will have to assist human fingers'

movements. It will have a greater capacity to propose rehabilitation tools for different pathologies and at different rehabilitation stages. The force tests shown in Fig. 6.15 show that the force generated by the two types of actuators flexion is very similar. Regardless of the efficiency, this force value is achieved with the same pressure value used in the previous experiment.

Similarly, the results of the force tests are analyzed in these cases. For this type of application, the desired results are the higher force values. The reason for this is that the more force the actuator can generate, the more possibilities it will have to assist human fingers' movements. It will have a greater capacity to create therapies for different types of pathologies and at different rehabilitation stages. The force tests shown in Fig. 6.15 show that the force generated by the two types of actuators in flexion is very similar, so there would not be a key factor to decide which one is better.

The only notable difference in these results is the deviation of the results. In this case, the textile actuators generate the most stable values. Analyzing the blocked force test results shows that the type of actuator that generates more force is the textile actuator (30% more than the silicone actuators). This result is essential for selecting the actuator type if an assistive device is to be built. Based on these experiments' results, it is suggested to select textile actuators with pleats to develop assistive or rehabilitative hand devices. As they meet the basic requirements in terms of force, they can be actuated without requiring much pneumatic energy, and the construction time is shorter than silicone actuators.

6.3   Actuators for Assistive Applications

Proper selection of actuation for an application in biomedical fields is a critical task in engineering. The design involves understanding the fundamental variables to be considered and how to characterize them on a test bench. The next step after measuring the device's performance consists of applying the technology in an actual scenario considering the trials executed during the characterization process. In this sense, it is possible to determine the device's capabilities and guarantee the safe human–robot interaction. This section presents assistive devices based on pneumatic actuation used and evaluated in clinical fields.

Based on the tests performed to characterize the types of soft actuators, the textile-type actuator was selected to construct rehabilitation and assistive device. The device was built using bending and extension actuators in the thumb and index finger. With these two actuators, it is possible to assist in the type of grip called the pincer grip, which was evaluated through the modified Jebsen Taylor test [35]. Figure 6.16 shows the device built with the textile actuators previously characterized and compared with the silicone actuators.

The Jebsen Taylor test consists of a series of 7 subtests to assess various hand functions related to activities of daily living. The subtests include tasks such as writing, turning letters, and picking up small objects. In the study conducted to evaluate the device's functionality, an adaptation of the test based on measuring the

Fig. 6.16 Front and side
view of the implementation of
the textile-type actuator in a
glove for the creation of the
assistive and rehabilitative
hand device

times required to hold different objects was used [36]. Five objects were selected
for this evaluation; a coin, an eraser, a sphere, a plastic cup, and a book. The test
compared the time required to hold each object without the device in a healthy
subject. The study results show that the device can assist in the grasping of objects
for activities of daily living. However, it is less efficient with small objects than with
large objects. In the healthy subject, the time to grasp everyday objects is higher
with the use of the device than without its use.

In the literature review, different hand rehabilitation devices based on wearable
robotics and soft robotics techniques were found. The technique based on pneumatic
actuators has been the most varied over the years. Initially, this style's devices began
using silicone actuators of the PneuNets type due to their ease of construction and
modeling. For example, a flexing glove with PneuNets actuators was built with
the ability to control the velocity and position of each actuator by pressure input
to the system [37]. In parallel, exoskeleton designs with other types of silicon
actuators were realized. For example, the development of an exoskeleton with
fiber reinforced actuators was evaluated in rehabilitation therapy [23]. Specifically,
fiber reinforced-type silicone actuators are most commonly used to construct these
assistive and rehabilitative hand devices. An exoskeleton for rehabilitation and task-
specific training help to perform tasks faster and more accurately in a subject with
stroke [23]. In this work, each actuator has different stretches of movement, which
allows the actuator to generate assistance in finger flexion and twist these. Another
exoskeleton built with fiber reinforced actuators was presented in [38]. The actuators
assisted finger flexion and were tested by inflating and deflating the actuators at 100
kPa to see each actuator's life cycle. Specifically, these actuators functioned properly
for 62.2 cycles of the previous test. Following the previous works, with the same
fiber reinforced silicone actuator, an exoskeleton was made for hand rehabilitation
that assists in flexion and extension movements. This movement is achieved with a
brace that generates a torque on the actuators that keeps them extended until they are
pressed for flexion. It is important to note that each actuator in this device weighs

37 g, which is a factor for improvement in future versions. This device was tested in a study with stroke patients.

On the side of exoskeletons built with textile-type actuators, the devices usually assist in both directions through layers of fabrics of different properties. For example, an exoskeleton for hand rehabilitation and assistance was built with corrugated textile actuators with the possibility to assist in both flexion and extension movements. This device's manufacture is particular because it is not made with elastic elements such as lycra-type fabrics. In this case, flexible materials such as TPU-coated fabric are used, and employing the geometry in some actuator layers, the flexion and extension movements are achieved. Also, in the study, a control interface is designed to switch between different operation modes such as specific tasks, bilateral rehabilitation, and grip types, among others [39]. With some external improvements in the device, a functionality study was performed based on the box and block test. It was found that the device assists in finger flexion, but the force generated in extension is not enough for patients with high muscle spasticity [20].

A fabric exoskeleton was built using the previous case's geometrical principles but with elastic materials such as lycra. That study uses textile actuators with pleats that facilitate the bending motion and reduce the input pressure. The designed device can assist in opening and closing the hand and was validated utilizing muscle activity in the forearm when performing the movements with and without the exoskeleton. Muscle activity in these tasks with the device is lower than without the exoskeleton [34]. Another following work [40] added force and deflexion sensors; bending actuators segmented by phalanges also were modified to apply force on only the parts needed. In this version of the device, the system requires 25 psi of power and can generate three movements; power closure, gripper closure, and finger extension. For evaluating the device, grip strength tests were performed, which obtained an 87% increase using the device. The Jebsen Hand Function Test and Box and Blocks tests evidenced improvements in patients with high-level injuries and reduced functionality in low-level injuries.

6.4 Conclusions

The characterization of actuators has several steps to fully understanding the capacities and limitations required for the aimed application. The test bench is the forefront tool to assess the actuator's performance through essential variables, depending on the implemented mechanical principles. This chapter presented the characterization process for two actuator types (i.e., variable stiffness actuator and pneumatic actuator) regarding the goal application and interaction scenario. Thus, the overall process defined the interesting variables, signals applied, and setup proposed to assess the actuator coupled in an assistive robot in terms of system response and device capabilities.

References

1. M.D.C. Sanchez-Villamañan, J. Gonzalez-Vargas, D. Torricelli, J.C. Moreno, J.L. Pons, Compliant lower limb exoskeletons: a comprehensive review on mechanical design principles. J. NeuroEng. Rehabil. **16**(1), 1–16 (2019)
2. J. Fang, J. Yuan, M. Wang, L. Xiao, J. Yang, Z. Lin, P. Xu, L. Hou, Novel accordion-inspired foldable pneumatic actuators for knee assistive devices. Soft Robot. **7**(1) 95–108 (2020)
3. M. Moltedo, G. Cavallo, T. Baček, J. Lataire, B. Vanderborght, D. Lefeber, C. Rodriguez-Guerrero, Variable stiffness ankle actuator for use in robotic-assisted walking: control strategy and experimental characterization. Mech. Mach. Theory **134**, 604–624 (2019)
4. M.B. Yandell, B.T. Quinlivan, D. Popov, C. Walsh, K.E. Zelik, Physical interface dynamics alter how robotic exosuits augment human movement: implications for optimizing wearable assistive devices. J. NeuroEng. Rehabil. **14**(1), 1–11 (2017)
5. J.-M. Belda-Lois, S. Mena-del Horno, I. Bermejo-Bosch, J.C. Moreno, J.L. Pons, D. Farina, M. Iosa, M. Molinari, F. Tamburella, A. Ramos, et al., Rehabilitation of gait after stroke: a review towards a top-down approach. J. Neuroeng. Rehabil. **8**(1), 66 (2011)
6. P.K. Jamwal, S. Hussain, S.Q. Xie, Review on design and control aspects of ankle rehabilitation robots. Disabil. Rehabil. Assist. Technol. **10**, 93–101 (2013)
7. M. Moltedo, T. Baček, B. Serrien, K. Langlois, B. Vanderborght, D. Lefeber, C. Rodriguez-Guerrero, Walking with a powered ankle-foot orthosis: the effects of actuation timing and stiffness level on healthy users. J. Neuroeng. Rehabil. **17**(1), 1–15 (2020)
8. Y. Li, K.A. Shorter, E.T. Hsiao-Wecksler, T. Bretl, Simulation and experimental analysis of a portable powered ankle-foot orthosis control, in *ASME 2011 Dynamic Systems and Control Conference and Bath/ASME Symposium on Fluid Power and Motion Control, DSCC 2011*, vol. 1(1), 77–84 (2011)
9. M. Moltedo, T. Bacek, K. Langlois, K. Junius, B. Vanderborght, D. Lefeber, Design and experimental evaluation of a lightweight, high-torque and compliant actuator for an active ankle foot orthosis, in *2017 International Conference on Rehabilitation Robotics (ICORR)* (IEEE, New York, 2017), pp. 283–288
10. Y.-L. Park, B.-R. Chen, D. Young, L. Stirling, R.J. Wood, E. Goldfield, R. Nagpal, Bio-inspired active soft orthotic device for ankle foot pathologies, in *2011 IEEE/RSJ International Conference on Intelligent Robots and Systems* (IEEE, New York, 2011), pp. 4488–4495
11. M. Manchola, D. Serrano, D. Gómez, F. Ballen, D. Casas, M. Munera, C.A. Cifuentes, T-FLEX: variable stiffness ankle-foot orthosis for gait assistance, in *Wearable Robotics: Challenges and Trends*, ed. by J. González-Vargas, J. Ibáñez, J.L. Contreras-Vidal, H. van der Kooij, J.L. Pons. Biosystems & Biorobotics (Springer International Publishing, New York, 2017), pp. 160–164
12. J. Casas, A. Leal Junior, C. Díaz, A. Frizera, M. Munera, C.A. Cifuentes, Large-range polymer optical-fiber strain-gauge sensor for elastic tendons in wearable assistive robots. Materials **12**, 1443 (2019)
13. D. Gomez-Vargas, M.J. Pinto-Bernal, F. Ballen-Moreno, M. Munera, C.A. Cifuentes, Therapy with t-flex ankle-exoskeleton for motor recovery: a case study with a stroke survivor, in *8th IEEE RAS & EMBS International Conference on Biomedical Robotics and Biomechatronics (BioRob)* (2020)
14. M.D. Manchola, M.J. Bernal, M. Munera, C.A. Cifuentes, Gait phase detection for lower-limb exoskeletons using foot motion data from a single inertial measurement unit in hemiparetic individuals. Sensors (Switzerland) **19**(13), 2988 (2019)
15. D. Gomez-Vargas, F. Ballen-Moreno, P. Barria, R. Aguilar, J. M. Azorín, M. Munera, C.A. Cifuentes, The actuation system of the ankle exoskeleton t-flex: first use experimental validation in people with stroke. Brain Sci. **11**(4), 412 (2021)
16. ASTM C1557-14, *Standard Test Method for Tensile Strength and Young's Modulus of Fibers* (ASTM International, West Conshohocken, PA, 2014)
17. G. Agarwal, N. Besuchet, B. Audergon, J. Paik, Stretchable materials for robust soft actuators towards assistive wearable devices. Sci. Rep. **6**(1), 1–8 (2016)

18. D. Bruder, B. Gillespie, C.D. Remy, R. Vasudevan, Modeling and control of soft robots using the Koopman operator and model predictive control (2019). Preprint. arXiv:1902.02827
19. H.K. Yap, J.H. Lim, F. Nasrallah, J. Cho Hong Goh, C.-H. Yeow, Characterisation and evaluation of soft elastomeric actuators for hand assistive and rehabilitation applications. J. Med. Eng. Technol. **40**(4), 199–209 (2016)
20. H.K. Yap, F. Sebastian, C. Wiedeman, C.-H. Yeow, Design and characterization of low-cost fabric-based flat pneumatic actuators for soft assistive glove application, in *2017 International Conference on Rehabilitation Robotics (ICORR)* (IEEE, 2017), pp. 1465–1470
21. M. Pozzi, E. Miguel, R. Deimel, M. Malvezzi, B. Bickel, O. Brock, D. Prattichizzo, Efficient fem-based simulation of soft robots modeled as kinematic chains, in *2018 IEEE international conference on robotics and automation (ICRA)* (IEEE, New York, 2018), pp. 4206–4213
22. E. Coevoet, A. Escande, C. Duriez, Soft robots locomotion and manipulation control using FEM simulation and quadratic programming, in *2019 2nd IEEE International Conference on Soft Robotics (RoboSoft)* (IEEE, 2019), pp. 739–745
23. P. Polygerinos, K.C. Galloway, E. Savage, M. Herman, K. O'Donnell, C.J. Walsh, Soft robotic glove for hand rehabilitation and task specific training, in *2015 IEEE International Conference on Robotics and Automation (ICRA)* (IEEE, New York, 2015), pp. 2913–2919
24. H.A. Varol, S.A. Dalley, T.E. Wiste, M. Goldfarb, Biomimicry and the design of multigrasp transradial prostheses, in *The Human Hand as an Inspiration for Robot Hand Development* (Springer, New York, 2014), pp. 431–451
25. P. Polygerinos, S. Lyne, Z. Wang, L.F. Nicolini, B. Mosadegh, G.M. Whitesides, C.J. Walsh, Towards a soft pneumatic glove for hand rehabilitation, in *2013 IEEE/RSJ International Conference on Intelligent Robots and Systems* (IEEE, New York, 2013), pp. 1512–1517
26. K.C. Galloway, P. Polygerinos, C.J. Walsh, R.J. Wood, Mechanically programmable bend radius for fiber-reinforced soft actuators, in *2013 16th International Conference on Advanced Robotics (ICAR)* (IEEE, New York, 2013), pp. 1–6
27. P. Polygerinos, Z. Wang, J.T. Overvelde, K.C. Galloway, R.J. Wood, K. Bertoldi, C.J. Walsh, Modeling of soft fiber-reinforced bending actuators. IEEE Trans. Robot. **31**(3), 778–789 (2015)
28. M. Ariyanto, J.D. Setiawan, R. Ismail, I. Haryanto, T. Febrina, D.R. Saksono, Design and characterization of low-cost soft pneumatic bending actuator for hand rehabilitation, in *2018 5th International Conference on Information Technology, Computer, and Electrical Engineering (ICITACEE)* (IEEE, 2018), pp. 45–50
29. Y. Sun, X. Liang, H.K. Yap, J. Cao, M.H. Ang, R.C.H. Yeow, Force measurement toward the instability theory of soft pneumatic actuators, IEEE Robot. Autom. Lett. **2**(2), 985–992 (2017)
30. J. Peters, E. Nolan, M. Wiese, M. Miodownik, M. Spurgeon, A. Arezzo, A. Raatz, H. Wurdemann, Actuation and stiffening in fluid-driven soft robots using low-melting-point material, in *Proceedings of the 2019 IEEE/RSJ International Conference on Intelligent Robots and Systems (IROS 2019)*, vol. 2019 (IEEE, New York, 2019)
31. C. Correia, K. Nuckols, D. Wagner, Y.M. Zhou, M. Clarke, D. Orzel, R. Solinsky, S. Paganoni, C.J. Walsh, Improving grasp function after spinal cord injury with a soft robotic glove. IEEE Trans. Neural Syst. Rehabil. Eng. **28**(6), 1407–1415 (2020)
32. K.H. Heung, R.K. Tong, A.T. Lau, Z. Li, Robotic glove with soft-elastic composite actuators for assisting activities of daily living. Soft Robot. **6**(2), 289–304 (2019)
33. P. Maeder-York, T. Clites, E. Boggs, R. Neff, P. Polygerinos, D. Holland, L. Stirling, K. Galloway, C. Wee, C. Walsh, Biologically inspired soft robot for thumb rehabilitation. J. Med. Dev. **8**(2) (2014)
34. L. Cappello, K.C. Galloway, S. Sanan, D.A. Wagner, R. Granberry, S. Engelhardt, F.L. Haufe, J.D. Peisner, C.J. Walsh, Exploiting textile mechanical anisotropy for fabric-based pneumatic actuators. Soft Robot. **5**(5), 662–674 (2018)
35. A. Peñas, J. Maldonado, O. Ramos, M. Munera, P. Barria, M. Moazen, H.A. Wurdemann, C.A. Cifuentes, Towards a fabric-based soft hand exoskeleton for various grasp taxonomies, in *The International Symposium on Wearable Robotics (WeRob2020) and WearRAcon Europe* (2020)
36. P. Tran, S. Jeong, S.L. Wolf, J.P. Desai, Patient-specific, voice-controlled, robotic FLEXotendon Glove-II system for spinal cord injury. IEEE Robot. Autom. Lett. **5**(2), 898–905 (2020)

37. M. Haghshenas-Jaryani, R.M. Patterson, N. Bugnariu, M.B. Wijesundara, A pilot study on the design and validation of a hybrid exoskeleton robotic device for hand rehabilitation. J. Hand Therapy **33**(2), 198–208 (2020)
38. Y. Jiang, D. Chen, J. Que, Z. Liu, Z. Wang, Y. Xu, Soft robotic glove for hand rehabilitation based on a novel fabrication method, in *2017 IEEE International Conference on Robotics and Biomimetics (ROBIO)*, pp. 817–822 (IEEE, New York, 2017)
39. H.K. Yap, P.M. Khin, T.H. Koh, Y. Sun, X. Liang, J.H. Lim, C.-H. Yeow, A fully fabric-based bidirectional soft robotic glove for assistance and rehabilitation of hand impaired patients. IEEE Robot. Autom. Lett. **2**(3), 1383–1390 (2017)
40. Y.M. Zhou, D. Wagner, K. Nuckols, R. Heimgartner, C. Correia, M. Clarke, D. Orzel, C. O'Neill, R. Solinsky, S. Paganoni, et al., Soft robotic glove with integrated sensing for intuitive grasping assistance post spinal cord injury, in *2019 International conference on robotics and automation (ICRA)* (IEEE, New York, 2019), pp. 9059–9065